

Supplementary information

Estimation of maximum AQP0 domains deformation from thin plate theory

The deformation of AQP0 thin junction domains increased with domain size (Figs. 4B and S2F). The maximum deformation was modeled assuming a flat circular plate of radius r and thickness h loaded at the center with a constant force (F) and clamped at the edges¹⁻³. The deflection (y) of the plate as a function of applied force and distance to the border (ρ) is

$$y(F, \rho) = \frac{3F(1-\nu^2)}{2\pi Eh^3} \left[\frac{1}{2}(r^2 - \rho^2) - \rho^2 \log\left(\frac{r}{\rho}\right) \right] \quad (\text{S1})$$

The maximum deflection (y_{\max}) is experienced at the center of the plate ($\rho=0$), thus

$$y_{\max}(F) = \frac{3F(1-\nu^2)}{4\pi Eh^3} r^2 = \frac{r^2}{16\pi D} F \quad (\text{S2})$$

where we have defined the flexural rigidity

$$D = \frac{Eh^3}{12(1-\nu^2)} \quad (\text{S3})$$

where E is the Young's modulus; and ν , the Poisson ratio, assumed 0.5.

To calculate the values of y_{\max} as a function the size (diameter) of AQP0 domain shown in Fig. 4B, we used $E = 58$ MPa, the value obtained from EC, single layer AQP0 measurements; and $t = 10$ nm, the thickness of a double layer AQP0 forming the thin junction. The applied force $F = 350$ pN, was the PeakForce imaging set point.

The expected maximum deformation of AQP0 domains from a difference in pressure (p) between two neighboring cells was computed from¹

$$y_{\max}(p) = \frac{r^2}{64D} p \quad (\text{S4})$$

In the main text, we assumed a pressure 20 kPa (the Young's modulus of nuclear fiber cells⁴).

Estimation of bending stiffness for lens membrane supramolecular structures

The bending stiffness of the various supramolecular structures of the lens membranes was determined using the above definition of flexural rigidity (equivalent to the bending stiffness, Eq. S3) and the reported elasticity and thickness measurements (table S1).

In the case of lipids domains, the bending stiffness was calculated using the slightly different formula proposed by Rawicz *et al.*⁵

$$\kappa_c = \frac{Eh^3}{24(1-\nu^2)} \quad (\text{S5})$$

which is half as rigid than assuming the two lipid monolayers being bonded (Eq. S3).

It is important to note that the values of the Young's modulus measured on the cytoplasmic side (in the double-layered membrane) are only valid for the connexin gap junctions, as these are the only structure supported on the mica substrate. The cytoplasmic AQP0 thin junction and the lipid regions were interpreted as being only supported by the edges. Thus the Young's moduli of AQP0 and lipids on the cytoplasmic side provide only a qualitative estimate of the flexibility of the structure, as discussed in the main text.

Table S1. Bending stiffness of lens membrane supramolecular structures

Structure		<i>E</i> (MPa)	<i>h</i> (nm)	κ_c ($k_B T$)
Lipid domains	Single layer	26	4.5	32 [#]
	Double layer		9	257 [#]
AQP0 domains	Single layer	58 [*]	5	195 ^{##}
	Double layer		10	1560 ^{##}
Cx domains	Single layer	56 ^{**}	6.5	415 ^{##}
	Double layer		13	3316 ^{##}

^{*} Measured from the extracellular side

^{**} Average between cytoplasmic and extracellular sides

[#] Using Eq. S5

^{##} Using Eq. S3

Supplementary figure legends

Supplementary figure S1. A) Derivation of the mechanical parameters from force-distance curves. The dashed grey line shows the maximum force of the setpoint during PeakForce imaging. The red line represents the range of the curve used to extract the elastic modulus (from the 5% to the 70% of the PeakForce setpoint). The blue horizontal arrow indicates the range of the contact region used to determine the deformation (from the 15% to 100% of the PeakForce setpoint). B) Representative approach (dashed lines) and retract (solid lines) force-distance curves acquired on EC lipid, EC AQP0, EC connexons and mica.

Supplementary figure S2. Calculation of undeformed topography images on the double layer lens membrane. A) Raw topography, B) deflection contact mode image of the EC surface, C) undeformed topography (topography + deformation), D) deformation. The most deformable regions appear darker (in A) in the deformed image and brighter in the undeformed one (C). Bar scale was 100 nm. False color scale was 30 nm for topography and topography+deformation and 1.1 nm for deflection. E) Line plots showing cross-sections along the dashed lines for the deformed (dotted) and undeformed (solid) images. F) Average deformation of AQP0 domains as a function of the diameter of the domains.

Supplementary figure S3. Left column shows the histograms (black lines) of the logarithm of the Young's modulus values ($\log(E)$) of the masked regions shown in the middle column images of $\log(E)$. The red lines are best fits to bimodal Gaussian distributions. The results of the fits are shown in table 1 in the main text. Masked regions presenting extracellular and cytoplasmic of either aquaporin 0 or connexin domains. The right column shows the topography of the same region. False color scales were the same for all $\log(E)$ and topography images.

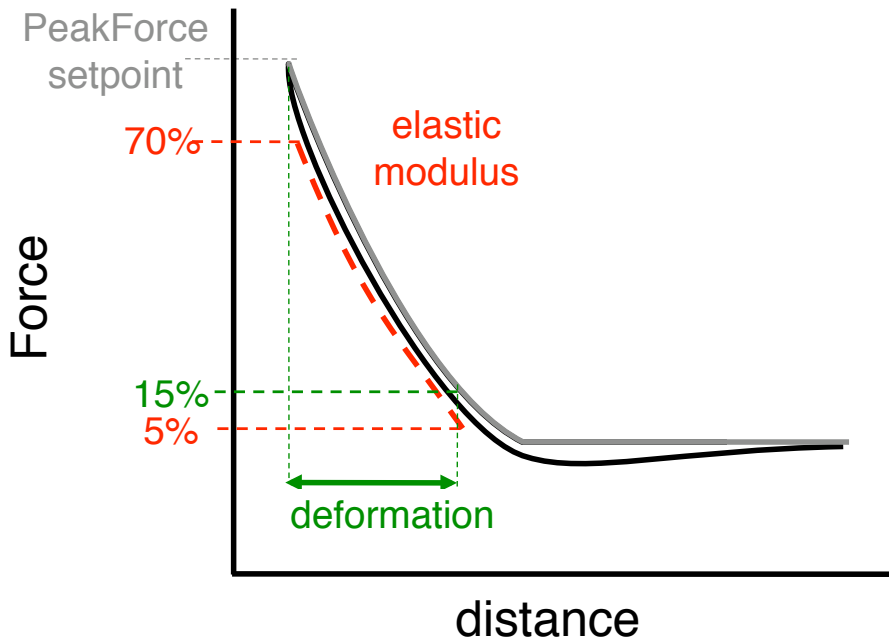
Supplementary figure S4. Reproduction of fig. 2 in the main text with the contact mode deflection image after nanodissection (D) shaded in yellow for lipid and dark blue for AQP0 domains. Non-shaded or light blue-circled regions represent connexon domains.

Supplementary figure S5. Deflection images of an AQP0 domain on the top layer (left, PeakForce) and of the same domain on the bottom layer after nanodissection (right, contact mode) revealing the same orientation of the AQP0 square lattice.

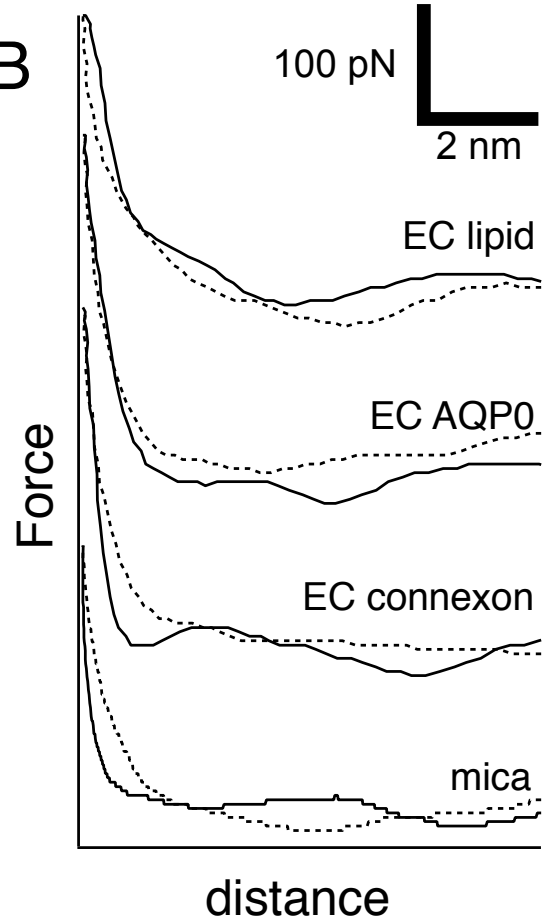
References

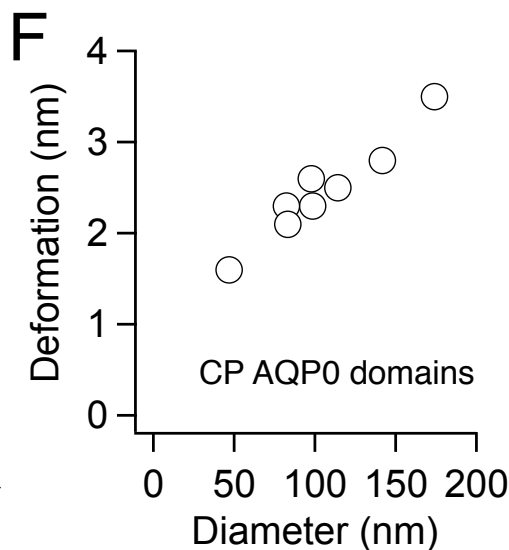
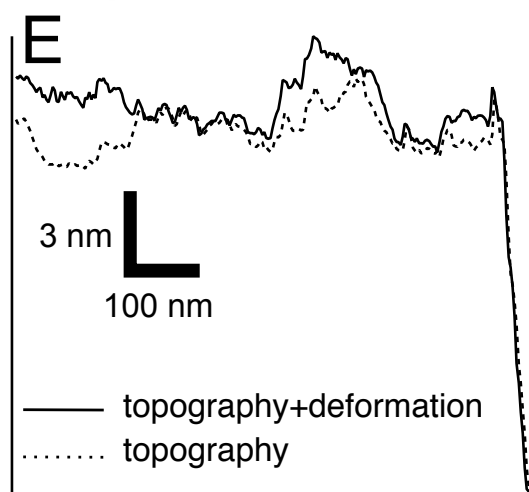
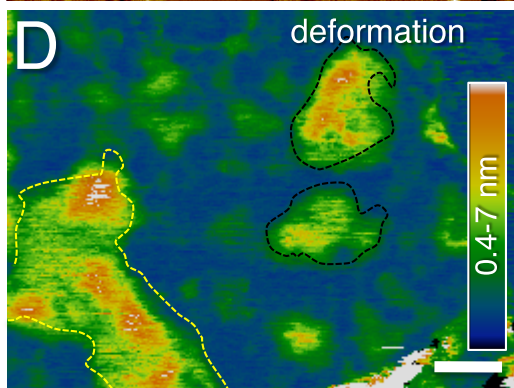
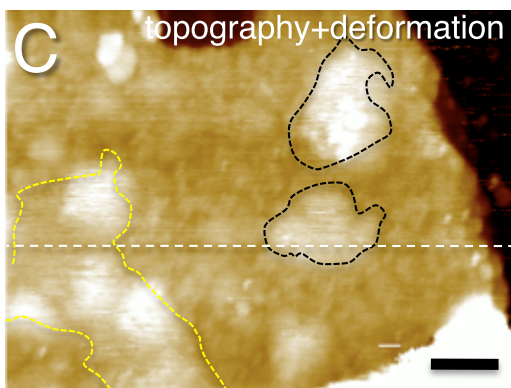
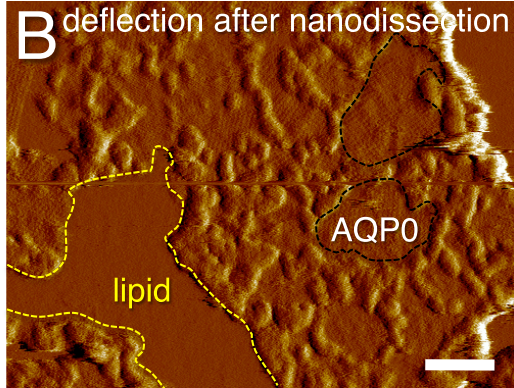
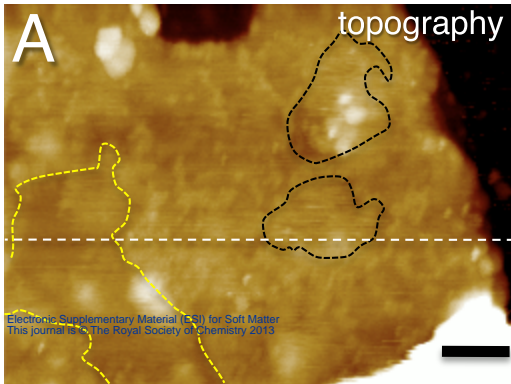
1. W. Young and R. Budynas, *Roark's Formulas for Stress and Strain*, McGraw-Hill Companies, Incorporated, 2001.
2. L. D. Landau and E. M. Lifshitz, *Theory of Elasticity*, Pergamon Press, Oxford, 1986.
3. I. Mey, M. Stephan, E. K. Schmitt, M. M. Müller, M. Ben Amar, C. Steinem and A. Janshoff, *J. Am. Chem. Soc.*, 2009, **131**, 7031-7039.
4. A. Hozic, F. Rico, A. Colom, N. Buzhynskyy and S. Scheuring, *Invest. Ophthalmol. Vis. Sci.*, 2012, **53**, 2151-2156.
5. W. Rawicz, K. C. Olbrich, T. McIntosh, D. Needham and E. Evans, *Biophys. J.*, 2000, **79**, 328-339.

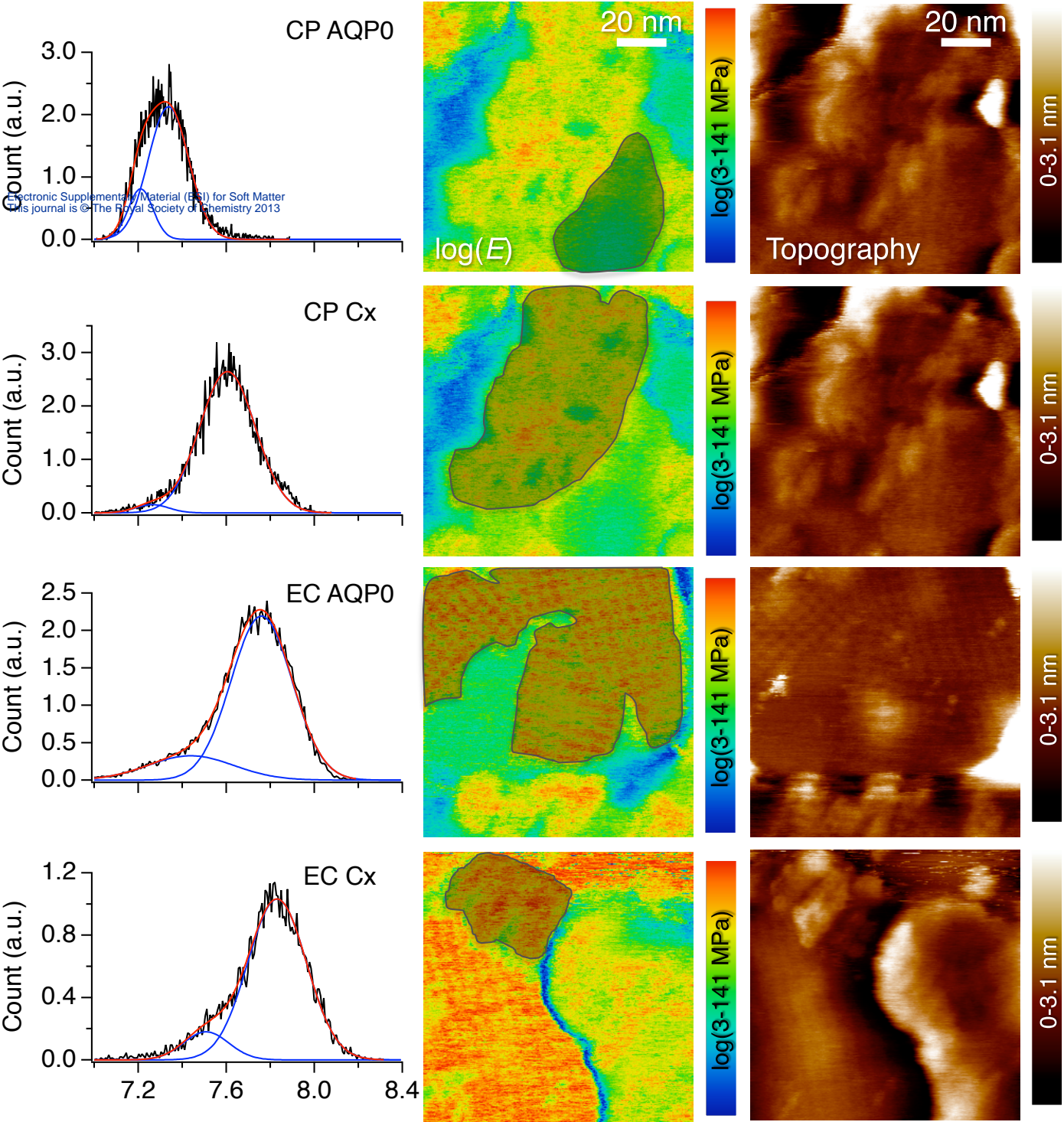
A

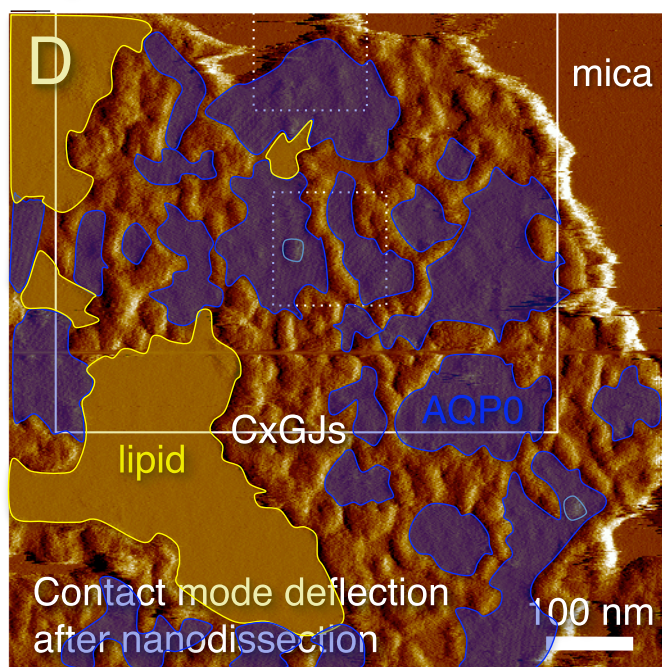
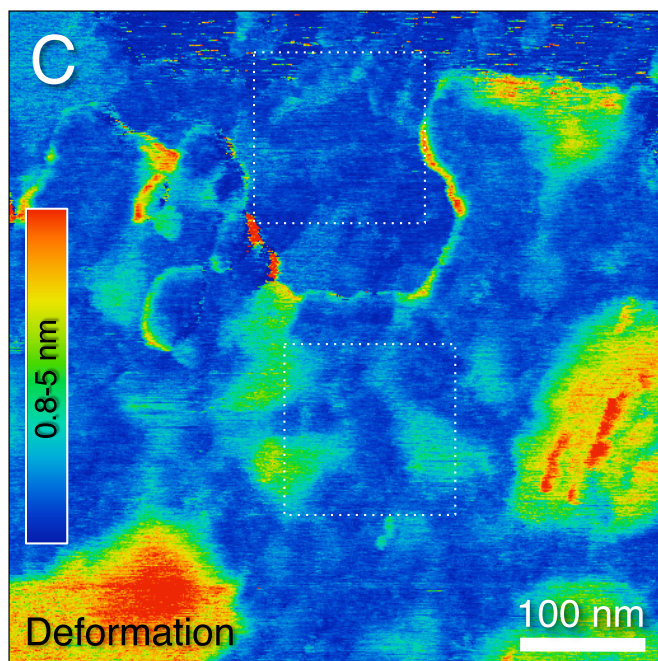
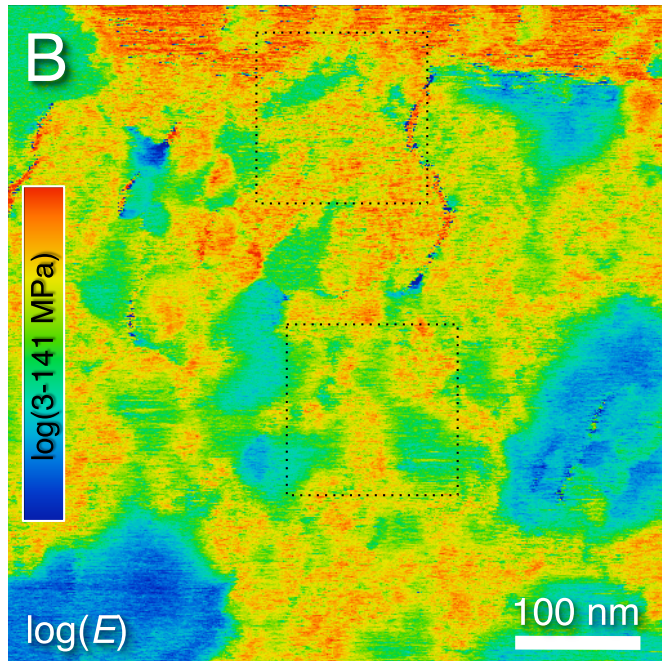
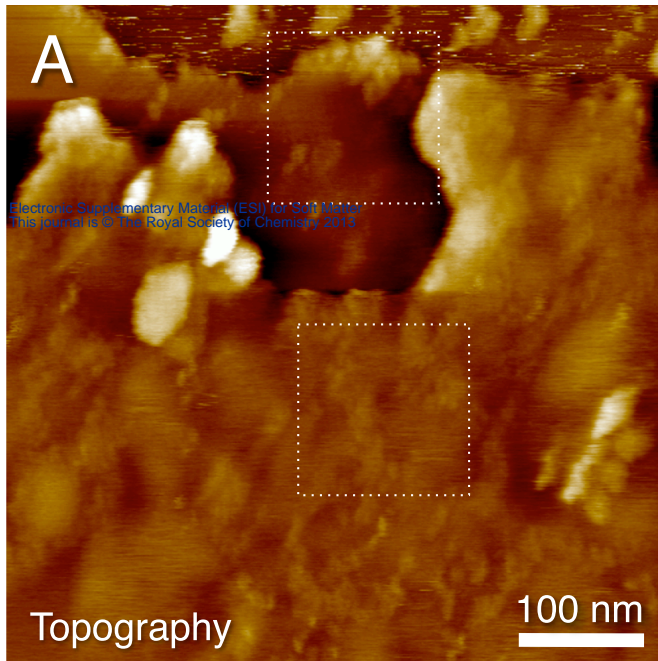


B

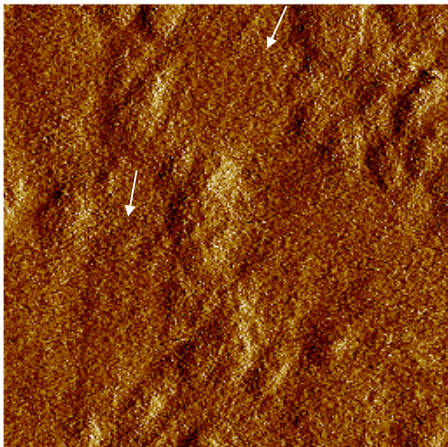








Peak force deflection on top layer



Contact mode deflection on bottom layer after dissection

